

U. of Iowa 97-2501; CERN 97-251

A Guide to Precision Calculations in Dyson's Hierarchical Scalar Field Theory

J. J. Godina

*Dep. de Fis. , CINVESTAV-IPN , Ap. Post. 14-740, Mexico, D.F. 07000
and*

Dpt. of Physics and Astr., Univ. of Iowa, Iowa City, Iowa 52246, USA

Y. Meurice* and M. B. Oktay*

CERN, 1211 Geneva 23, Switzerland

and

Dpt. of Physics and Astr., Univ. of Iowa, Iowa City, Iowa 52246, USA

S. Niermann

Dpt. of Physics and Astr., Univ. of Iowa, Iowa City, Iowa 52246, USA

Abstract

The goal of this article is to provide a practical method to calculate, in a scalar theory, accurate numerical values of the renormalized quantities which could be used to test any kind of approximate calculation. We use finite truncations of the Fourier transform of the recursion formula for Dyson's hierarchical model in the symmetric phase to perform high-precision calculations of the unsubtracted Green's functions at zero momentum in dimension 3, 4, and 5. We use the well-known correspondence between statistical mechanics and field theory in which the large cut-off limit is obtained by letting β reach a critical value β_c (with up to 16 significant digits in our actual calculations). We show that the round-off errors on the magnetic susceptibility grow like $(\beta_c - \beta)^{-1}$ near criticality. We show that the systematic errors (finite truncations and volume) can be controlled with an exponential precision and reduced to a level lower than the numerical errors. We justify the use of the truncation for calculations of the high-temperature expansion. We calculate the dimensionless renormalized coupling constant corresponding to the 4-point function and show that when $\beta \rightarrow \beta_c$, this quantity tends to a fixed value which can be determined accurately when $D = 3$ (hyperscaling holds), and goes to zero like $(Ln(\beta_c - \beta))^{-1}$ when $D = 4$.

PACS: 05.50.q, 11.10.Hi, 11.10.Kk, 11.15.Tk, 64.60.Fr, 74.40.Cx, 75.40.Gb

Typeset using REVTeX

I. INTRODUCTION

Finding closed form, exact analytical solutions to difficult problems is considered as a great achievement in theoretical physics. In recent years, the development of fast computers and of easy electronic communications has enlarged the class of solutions which can be considered as completely satisfactory. Lengthy expressions can be manipulated symbolically or numerically and communicated to others (for a concrete example, see for instance the Appendices of Ref. [1]). Sometimes, the solution of a problem requires a combination of iterations and expansions which can be performed with any desirable precision in a short amount of time using a friendly environment such as *Mathematica*. An example of such a solution is the calculation of the spectrum of the one-dimensional quantum anharmonic oscillator described in Ref. [2]. In this example, even though no closed expression for the eigenvalues and eigenfunctions is available, the beginning of the spectrum can be obtained numerically with great precision and almost instantly using *Mathematica*. We could say that this problem is numerically solvable.

Scalar field theory on a Euclidean lattice is a difficult problem with many important applications, such as the interactions of strongly interacting light particles (pions, kaons,...), the generation of mass in the standard model of elementary particles, and the theory of critical phenomena. The renormalization group method [3] helps us to understand the nature of the continuum limit [4] for such a model. However, in the case of short range (nearest neighbor) interactions, we are still far away from the numerical solvability mentioned above.

In order to solve scalar field theory, one needs an approximation scheme such that: a) the zeroth-order approximation preserves the main qualitative features of the model, b) the zeroth-order approximation is analytically or numerically solvable, and c) the zeroth-order approximation can be improved systematically and in a practically implementable way. The fact that Wilson's approximate recursion formula satisfies the requirement a) is justified in Ref. [3]. The approximate recursion formula is an integral equation with one variable which can be handled by standard numerical methods. The main sources of errors are the finite number of points of integration and the parametrization of the behavior of the tails of the functions integrated. The errors can be reduced by reducing the size of the tails and increasing the number of points. We found this approach time consuming and inefficient. However, using the Fourier transform of the recursion formula, we found a natural approximate method with a fast implementation and a control of the systematic errors which is better than exponential. This method is the main calculational tool used and discussed in the present article.

The approximate recursion formula is closely related to the recursion formula appearing in Dyson's hierarchical model [5]. More precisely [6], at fixed dimension, there exists a one parameter family of recursion formulas which interpolates continuously between the two. Following Ref. [6], we call this parameter ζ . Seen from a practical point of view in our calculation, the extension to another value of ζ in the recursion formula amounts to changing one number in one line of a two page program. Physical quantities such as the critical exponents vary slowly when ζ is varied, but there is nothing that singles out a particular value of ζ . In the following, we specialize the discussion and the numerical study to the case of Dyson's model ($\zeta = 1/D$) because this model has been studied [7–10] in great detail in the past. Dyson's model is a well-defined lattice model and it admits the same

kind of expansions (weak and strong coupling, large- N etc.) as any other scalar model on a cubic lattice. The basic recursion formula and the approximation methods are explained in section II.

For simplicity, all the calculations done below use an initial Ising measure. The infinite cut-off limit is obtained by fine-tuning the only adjustable parameter, namely, the inverse temperature β . All the results will be expressed in terms of $\beta_c - \beta$. The general procedure [3,4] which relates small values of $\beta_c - \beta$ to large values of the UV cut-off is well-known and will not be repeated here. From a calculational point of view, the discussion would be essentially the same if instead we had fixed $\beta = 1$ and considered initial measures depending on a cut-off and several bare parameters.

The rest of the presentation is based on the following empirical fact: the systematic errors due to finite volume fall exponentially with the number of iterations (n_{max} and the systematic errors due to finite dimensional truncation fall faster than exponentially with the dimension of the truncated space (l_{max}). In calculations involving double precision, one can, without encountering major difficulties, choose n_{max} and l_{max} in such a way that if we increase these parameters further, no change is observed in the results. One can then first determine the critical temperature and the numerical errors. We need to discuss these first, because the numerical errors are a fundamental limitation whenever the precision of the arithmetic operations is fixed, and there is no point in trying to reduce the systematic errors much below the numerical errors.

The phase structure of the approximated models is discussed in section III. We show that, for understandable reasons, there is nothing that can be identified as a low-temperature phase. We also give a practical method to identify the inverse of the critical temperature, denoted β_c , with an optimal accuracy. In the following sections, it will always be assumed that we work in the symmetric phase ($\beta < \beta_c$).

The numerical errors on the magnetic susceptibility are studied in section IV, where we show that the relative errors obey the approximate law

$$\left| \frac{\delta\chi}{\chi} \right| \sim \frac{\delta}{\beta_c - \beta}, \quad (1.1)$$

where δ is the precision used to perform the arithmetical operations. We also show that this law follows from an approximate renormalization group calculation. As a by-product we obtain a numerical estimate of the critical exponent γ in good agreement with the existing estimates [9–11] for $D = 3$. As a general remark, we have a much better quantitative control on the details of renormalization group arguments in $D = 3$ than in $D = 4$, where confluent logarithmic singularities make the analysis more delicate.

We then discuss the systematic errors. The volume dependence of the magnetic susceptibility is discussed in section V. We show that in order to calculate the susceptibility at an inverse temperature β , in D dimensions, and with relative errors Δ , one needs a number of lattice sites which is of the order of $(\Delta(\beta_c - \beta)^\gamma)^{-D/2}$. We then show that when the Fourier transform of the recursion formula of Dyson's hierarchical model is projected into a finite dimensional space of dimension l_{max} , the relative errors on the susceptibility associated with this truncation decrease faster than $e^{-a l_{max}}$ for some positive number a . We show in section VII that similar results apply to the high-temperature expansion of the susceptibility, justifying the procedure used in Ref. [10].

At this point, we have only discussed the susceptibility, or in other words, the 2-point function. The 4-point function is also provided by the calculational method at no extra cost. However, the calculation of the corresponding renormalized coupling constant requires a subtraction. In the discussion of the errors on the susceptibility, we have explained that while we are iterating the recursion formula we lose significant digits “from the right”. With the subtraction, we also lose significant digits “from the left”. This is explained in section VIII, where we calculate a “dimensionless coupling constant” inspired by the field theory definition of Ref. [12] and denoted λ_4 .

In the case $D = 3$, we show that when $\beta \rightarrow \beta_c$, λ_4 tends to a fixed non-zero value that we were able to calculate with 6 significant digits. This is very convincing evidence that hyperscaling holds for the model considered here. For the nearest-neighbor Ising model on a 3-dimensional cubic lattice, it is very hard to decide if hyperscaling holds on the basis of Monte-Carlo simulations [13] or high-temperature expansion [14]. In the present case, it is a short and straightforward calculation. This shows that it would be worth trying to interpolate perturbatively between Dyson’s model and nearest neighbor models, transforming the qualitative approximation [3] into a quantitative approximation. The accuracy of λ_4 decreases when D increases. However, we were able to obtain good evidence that in $D = 4$, λ_4 decrease like $(Ln(\beta_c - \beta))^{-1}$, in good agreement with the behavior obtained with the field theory method [15] at lowest order in perturbation theory.

Our results show that it is possible to calculate accurately, and without major effort, the renormalized quantities which can be extracted from the 2- and 4-point functions. These calculations can be done for an extended range of small values of $\beta_c - \beta$. In other words, for existing computers, requirement b) is fulfilled by the hierarchical approximation provided that one does not require too-small values of $\beta_c - \beta$. Numerical solvability can sometimes completely change our point of view regarding a problem. Taking the example of differential equations, at a time when their numerical solutions were not achievable, one could dream of a perfectly deterministic approach to natural phenomena in which everything could be known once the rules of evolution and the initial conditions were given.

This paper provides a calculational method to anyone who would like to check an approximation method with accurate numerical results. As explained above, most of the approximation schemes which apply to a scalar field theory with nearest neighbor interactions on a cubic lattice also apply to Dyson’s model. We are presently testing the validity of several well-known but not easy-to-control expansions: the renormalized perturbative expansion, the loop expansion, and the large- N expansion.

II. THE RECURSION FORMULA AND ITS FINITE DIMENSIONAL TRUNCATIONS

In this section, we briefly describe Dyson’s hierarchical model and the methods used to calculate the average of arbitrary powers of the zero momentum component of the scalar field. The models considered here have $2^{n_{max}}$ sites. We label the sites with n_{max} indices $x_{n_{max}} \dots x_1$, each index being 0 or 1. In order to visualize the meaning of this notation, one can divide the $2^{n_{max}}$ sites into two blocks, each containing $2^{n_{max}-1}$ sites. If $x_{n_{max}} = 0$, the site is in the first block, if $x_{n_{max}} = 1$, the site is in the second block. Repeating this procedure n_{max} times (for the two blocks, their respective two sub-blocks, etc.), we obtain

an unambiguous labeling for each of the sites. Two sites differing only by x_1 are in the same block of size 2. We write the action as

$$S = -\frac{1}{2} \sum_{n=1}^{n_{max}} \left(\frac{c}{4}\right)^n \sum_{x_{n_{max}}, \dots, x_{n+1}} \left(\sum_{x_n, \dots, x_1} \phi_{(x_{n_{max}}, \dots, x_1)} \right)^2 . \quad (2.1)$$

The index n , referred to as the “level of interaction” hereafter, corresponds to interactions of the total field in blocks of size 2^n . The free parameter c , controlling the strength of the interactions, is set equal to $2^{1-2/D}$ in order to approximate a nearest neighbor model in D -dimensions. In this article, we will consider the cases $D = 3, 4$, and 5 .

The field $\phi_{(x_{n_{max}}, \dots, x_1)}$ is integrated with a local measure $W_0(\phi)$ which needs to be specified. In the following, we use an Ising measure, $W_0(\phi) = \delta(\phi^2 - 1)$, which takes only the values ± 1 . To the best of our knowledge, the results presented do not depend on this specific choice and would also apply, for instance to the case of Landau-Ginzburg measures of the form $W_0(\phi) = e^{-A\phi^2 - B\phi^4}$.

The integrations can be performed iteratively using the recursion formula

$$W_{n+1}(\phi) = \frac{C_{n+1}}{2} e^{\frac{\beta}{2} \left(\frac{c}{4}\right)^{n+1} \phi^2} \int d\phi' W_n\left(\frac{\phi - \phi'}{2}\right) W_n\left(\frac{\phi + \phi'}{2}\right) , \quad (2.2)$$

where C_{n+1} is a normalization factor which can be fixed at our convenience. The relation between this recursion formula and Wilson’s approximate recursion formula [3] is discussed in Ref. [6]. Introducing the Fourier representation

$$W_n(\phi) = \int \frac{dk}{2\pi} e^{ik\phi} \widehat{W}_n(k) , \quad (2.3)$$

and a rescaling of the source k by a factor $1/s$ at each iteration, through the redefinition

$$R_n(k) = \widehat{W}_n\left(\frac{k}{s^n}\right) , \quad (2.4)$$

the recursion formula becomes [8]

$$R_{n+1}(k) = C_{n+1} \exp\left(-\frac{1}{2}\beta\left(\frac{c}{4}s^2\right)^{n+1} \frac{\partial^2}{\partial k^2}\right) (R_n\left(\frac{k}{s}\right))^2 . \quad (2.5)$$

The rescaling operation commutes with iterative integrations and the rescaling factor s can be fixed at our convenience.

In the following, we fix the normalization constant C_n in such way that $R_n(0) = 1$. $R_n(k)$ has then a direct probabilistic interpretation. If we call M_n the total field $\sum \phi_x$ inside blocks of side 2^n , and $\langle \dots \rangle_n$ the average calculated without taking into account the interactions of level strictly larger than n (or in other words, as if n were equal to n_{max}), we can write

$$R_n(k) = \sum_{q=0}^{\infty} \frac{(-ik)^{2q} \langle (M_n)^{2q} \rangle_n}{2q! s^{2qn}} . \quad (2.6)$$

We see that the Fourier transform of the local measure obtained after n iterations generates the zero-momentum Green’s functions calculated with 2^n sites, and can thus be used to calculate the renormalized coupling constants at zero momentum.

The choice of s is a matter of convenience. For calculations in the symmetric (high-temperature) phase not too close to the critical temperature, or for high-temperature expansions [8,9], the choice $s = \sqrt{2}$ works well. For calculations very close to the critical temperature, the choice $s = 2c^{-\frac{1}{2}}$ prevents the appearance of very large numbers. In the following calculations, we *always* use $s = 2c^{-\frac{1}{2}}$.

In the following, the finite volume magnetic susceptibility is defined as

$$\chi_n(\beta) = \frac{\langle (M_n)^2 \rangle_n}{2^n}. \quad (2.7)$$

With the rescaling $s = 2c^{-\frac{1}{2}}$, we have the relation

$$\chi_n = -2a_{n,1} \left(\frac{2}{c}\right)^n. \quad (2.8)$$

The initial condition for the Ising measure is $R_0 = \cos(k)$. For the Landau-Ginzburg measure, the coefficients in the k -expansion need to be evaluated numerically.

In previous publications [9,10], we used the β expansion of Eq. (2.5) to calculate the high-temperature expansion of the magnetic susceptibility of Dyson's hierarchical model up to order 800 with an Ising or a Landau-Ginzburg measure. The calculation of the large-order coefficients requires a lot of computing time. We found that using a truncation in the expansion in k^2 at order 50 could cut the computer time by a factor of order 100 while having effects on the values of the coefficients which were smaller than the errors due to numerical round-off.

We consider the finite dimensional approximations of degree l_{max} :

$$R_n(k) = 1 + a_{n,1}k^2 + a_{n,2}k^4 + \dots + a_{n,l_{max}}k^{2l_{max}}. \quad (2.9)$$

After each iteration, non-zero coefficients of higher order ($a_{n+1,l_{max}+1}$ etc.) are obtained, but not taken into account (i.e. set to zero as part of the approximation) in the next iteration. More explicitly, the recursion formula for the $a_{n,m}$ reads:

$$a_{n+1,m} = \frac{\sum_{l=m}^{l_{max}} (\sum_{p+q=l} a_{n,p} a_{n,q}) \frac{(2l)!}{(l-m)!(2m)!} \left(\frac{c}{4}\right)^l \left(-\frac{1}{2}\beta\right)^{l-m}}{\sum_{l=0}^{l_{max}} (\sum_{p+q=l} a_{n,p} a_{n,q}) \frac{(2l)!}{l!} \left(\frac{c}{4}\right)^l \left(-\frac{1}{2}\beta\right)^l}. \quad (2.10)$$

III. THE PHASE STRUCTURE OF THE APPROXIMATED MODELS

From a field theoretic point of view, an important feature of the hierarchical model is its second order phase transition. Our first task will be to identify β_c for the well-studied [9,16] case of an Ising measure. The truncation described above can be used to calculate [8] *exactly* the high-temperature expansion of the magnetic susceptibility up to order $l_{max} - 1$, and one can think about the truncation as a partially re-summed high-temperature expansion. It seems thus unlikely that when l_{max} becomes large, we would obtain sensible results when $\beta > \beta_c$. This guess is confirmed by empirical numerical experiments at fixed β .

The truncated recursion formula shows very clearly the existence of a high-temperature phase where for β smaller than β_c and n large enough, we have the scaling law

$$a_{n,1} \propto 2^{-\frac{2n}{D}} . \quad (3.1)$$

Given the choice of scaling factor $s = 2c^{-\frac{1}{2}}$ and the definition of c discussed in section II, this scaling is equivalent to the “central limit” behavior

$$\langle (M_n)^{2q} \rangle_n \propto 2^{nq} . \quad (3.2)$$

This situation is characterized by ratios $a_{n+1,1}/a_{n,1}$ reaching the value $c/2 = 2^{-\frac{2}{D}}$.

On the other hand, when β is increased sufficiently, there is a sudden change of behavior. However, there is nothing that we can identify with a low-temperature phase [12]. In all the cases that we have considered, the change is signaled by the fact that when n increases, the ratio $a_{n+1,1}/a_{n,1}$ becomes larger than 1, and then starts making unpredictable changes, *never* returning to any kind of behavior like Eq. (3.2) or the behavior characteristic of the low temperature phase, namely

$$\langle (M_n)^{2q} \rangle_n \propto 2^{n2q} . \quad (3.3)$$

The “irreversibility” of this process allows us to identify unambiguously β_c , in the sense that a calculation at finite n gives upper and lower bounds on β_c . By increasing n , we can obtain sharper bounds. This procedure is illustrated for $D = 3$ in Fig. 1.

We see that a calculation for n up to 50 allows us to resolve the 10-th digit of β_c , and a calculation for n up to 60 allows us to resolve the 11-th digit. Proceeding similarly, we can determine the numerical value of β_c with as many significant digits as the computational method allows. Double precision Fortran calculations made with $l_{max} = 80$ are reported below for the Ising model in 3, 4, and 5 dimensions. The results are in agreement with the bounds found in ref. [16] with independent (and exact) calculational methods. The third column gives the minimal value of n which allows a resolution of the 16 significant digits.

D	β_c	n_{min}	$l_{max_{min}}$
3	1.179030170446270	102	32
4	0.6654955715318593	111	43
5	0.4569633006170210	132	45

(3.4)

Subsequently, l_{max} was lowered by small steps until the value of β_c changed. This experiment shows that the change occurs at values much smaller than 80. In the fourth column of Table 1, we give the minimal value of l_{max} such that the stable value of β_c with 16 significant digits can be reached.

One may wonder if the precise value of β_c is dependent on the numerical aspects of the calculation such as the round-off errors, which will be discussed in the next section. To settle this question, we have used methods which perform the arithmetic operations differently (these methods are explained in detail in the next section) and found the very same values of β_c . In conclusion, we have found a reasonably robust value of β_c which is consistent with existing results.

We have calculated β_c^{-1} for dimensions much larger than 4. The results are displayed in Fig. 2. We see that this quantity grows linearly with the dimension. The explicit calculation of the high-temperature expansion [1] suggests that when $D \rightarrow \infty$, i.e. when $c \rightarrow 2$, we have

$$b_m \simeq \left(\frac{2c}{(4-c)(2-c)} \right)^m, \quad (3.5)$$

which implies that

$$\beta_c^{-1} \simeq \frac{D}{2Ln2}. \quad (3.6)$$

This estimate of the slope is in good agreement with the data. We found a slope of 0.714, while $(2Ln(2))^{-1} = 0.721$. Next we will study the various sources of error occurring when one approaches β_c from below.

IV. THE ROUND-OFF ERRORS

Round-off errors can play an important role when recursive methods are used, because they may grow faster than the improvement of the results due to the repeated use of the method. For this reason, we have studied them with three independent methods. By independent, we mean that the arithmetic is performed in a completely uncorrelated fashion.

We have compared our original Fortran calculation on a DEC-alpha with three other calculations. The first one was the same program run on a MIPS. The second one was a Mathematica program where a higher precision in the arithmetic operations was set. The precision was adjusted in such a way that the susceptibility was obtained correctly with 16 significant digits. Thirdly, we have compared the calculation with the one obtained with a slightly different rescaling, namely $s = 1.98c^{-\frac{1}{2}}$, a method already used in Ref. [9,10]. All these calculations were performed with $l_{max} = 60$, which is beyond what we need (see next section).

The relative differences in the finite volume susceptibility are shown in Fig. 3, for $D = 3$ and $\beta_c - \beta = 10^{-11}$. The figure shows clearly that the three types of discrepancies are essentially the same. Since the three types of errors are uncorrelated, we can identify them with the round-off errors and calculate them with the most convenient method. Using the third method, we have calculated the round-off errors for various values of β . In all the cases, the logarithm of the relative error grows linearly at the beginning and then stabilizes at a constant value. The period of linear growth corresponds roughly to the iterations where $\chi_{n+1} \simeq 2^{\frac{2}{D}} \chi_n$. For larger n , the value of the susceptibility stabilizes, with changes decreasing by a factor $2^{-\frac{2}{D}}$ at each step. During this second stage, the numerical errors do not grow significantly.

We now proceed to discuss the asymptotic values of the errors, in other words, the stable value they reach for n sufficiently large. We have collected these values for various temperatures and $D = 3, 4$, and 5 in Fig. 4. This shows that the relative error is in good approximation $10^{-16}(\beta_c - \beta)^{-1}$, independently of D .

These empirical results have a simple explanation in terms of the linearized theory. Suppose that δ is a typical round-off error in a calculation (e.g. 10^{-16}), and that λ is the largest eigenvalue of the linearized renormalization group transformation near a given fixed point. One expects the numerical error on $a_{n,1}$ to be of the order $\lambda^n \delta$. With the rescaling used in this paper, this means that the errors on the susceptibility are of the order

$$|\delta \chi_n| \sim \lambda^n \delta \left(\frac{2}{c} \right)^n. \quad (4.1)$$

Now for n such that $\lambda^n \sim (\beta_c - \beta)^{-1}$, we have $\chi \sim (\frac{2}{c})^n$. Plugging this into the previous equation, we get

$$\left| \frac{\delta\chi}{\chi} \right| \sim \frac{\delta}{\beta_c - \beta}, \quad (4.2)$$

which is the empirical result found above.

For $D = 3$, one can check the details of the above argument and, as a by-product, obtain an estimate of λ . The slope of the increasing part of Fig. 3 is approximately 0.154, with an estimated error of order 0.001. This implies a value $10^{0.154} = 1.427$ for λ . Using the usual formula for the critical exponent,

$$\gamma = \frac{Ln(\frac{2}{c})}{Ln(\lambda)}, \quad (4.3)$$

we obtain the value $\gamma = 1.30$, in good agreement with existing estimates [9–11].

For $D = 4$, the same procedure gives an exponent which is too high by about 3 percent (compared to the trivial value). This is a typical error when one does not take into account the marginal direction and the (related) confluent logarithmic singularity in the susceptibility.

V. VOLUME EFFECTS

In the two previous sections, we developed a qualitative understanding regarding the finite volume susceptibility χ_n , or in other words regarding the way the susceptibility depends on the number of iterations. Volume effects can be important in the determination of the critical exponents. For instance, in Ref. [16], *exact* calculation with almost a million sites gave errors of more than 10 percent in the exponent γ . We are now ready to get a better quantitative understanding of these effects.

If we consider the evolution of $\chi_n(\beta)$ when n increases, with β fixed slightly below β_c , we see from Fig. 1 that when we are close to the fixed point, $\chi_{n+1} \simeq 2^{\frac{2}{D}}\chi_n$. This lasts until the right order of magnitude ($\sim (\beta_c - \beta)^{-\gamma}$) is reached. For larger n , the value of the susceptibility stabilizes, with errors decreasing at each step. In this second regime, the measure becomes asymptotically Gaussian, and one can estimate the change in χ_n from the change in the k^2 term. From the basic formula (2.5), one gets the estimate for the relative change:

$$\Delta_n = \left| \frac{\chi_{n+1} - \chi_n}{\chi_n} \right| \propto 2^{-\frac{2}{D}n} \chi_n. \quad (5.1)$$

From these considerations, we find the number $n(\beta, \Delta)$ of iterations necessary to calculate the susceptibility at fixed β , with a relative precision Δ (defined as in Eq. (5.1)) :

$$n(\beta, \Delta) = -\left(\frac{DLn(10)}{2Ln(2)}\right)(Log_{10}(\Delta) + \gamma Log_{10}(\beta_c - \beta)). \quad (5.2)$$

The comparison with a numerical calculation where we required $\Delta = 10^{-15}$ is given in Fig. 5 for $D = 3, 4$, and 5. The agreement with the estimate of Eq. (5.2) with $\gamma = 1.3$ (1.0) for $D = 3$ (4 and 5), is quite good.

The fact that we were able to stabilize sixteen digits of the susceptibility does not mean that the results have sixteen digit accuracy. The asymptotic stability of the numerical results comes from the fact that the r. h. s. of Eq. (5.1) will go to zero whenever χ_n quits growing. This occurs independently of the fact that numerical errors may occur while χ_n builds up its bulk value. Consequently, a more realistic approach would be to require a precision consistent with the round-off errors discussed in the previous section. Imposing a temperature-dependent requirement $\Delta = 10^{-16}(\beta_c - \beta)^{-1}$, we obtain values of n shown in Fig. 5.

VI. CONTROLLING THE EFFECTS OF FINITE DIMENSIONAL TRUNCATIONS

In this section, we study the l_{max} dependence of the magnetic susceptibility for $\beta < \beta_c$. For notational purposes, we call $\chi^{(l)}$ the susceptibility corresponding to a given value $l_{max} = l$. For each calculation, the value of n_{max} has been increased until no change could be observed. The results are displayed in Fig. 6 for $\beta_c - \beta = 10^{-8}$. For low l , $\chi^{(l)}$ grows at a not-very regular rate and within the bounds $1 < \chi^{(l+1)}/\chi^{(l)} < 10$. When l gets close to 20, $\chi^{(l)}$ starts stabilizing with a precision which seems to be exponential. For instance, for $D = 3$, the relative errors fall approximately like $10^{-0.6l}$. This exponential rate is based on the assumption that the logarithm of the relative errors falls linearly. However, a closer look shows that it falls slightly faster. This is illustrated in Fig. 7. The best parametrization that we have found is a linear function times the logarithm of l . A more detailed analysis shows that this new parametrization reduces the square root of the sum of the square of the relative differences ((fit-data)/data) by one order of magnitude. This suggests that one should try to derive rigorous bounds where the errors are proportional to some inverse power of (l_{max} !).

We have thus studied the logarithm of the relative differences (due to the change in l_{max}) divided by the logarithm of l_{max} for various temperatures with $D = 3$. The results are shown in Fig. 7. We then used linear fits for the part falling linearly. In other words, we assumed the approximate law

$$\left| \frac{\chi^{l+1} - \chi^l}{\chi^l} \right| \simeq l^{(-|s|l+q)} . \quad (6.1)$$

The results can be summarized as follows. The slope is almost independent of β and takes the approximate value -0.41 with changes of order 0.01. The intercept grows linearly with $-Log_{10}(\beta_c - \beta)$, as shown in Fig. 9. A linear fit of this data gives an intercept of the form $1.7 - 0.83 \times Log_{10}(\beta_c - \beta)$. If we neglect the slow logarithmic variations and approximate it by a constant central value in the falling part of Fig. 8, we obtain the approximate law

$$\left| \frac{\delta\chi}{\chi} \right| \sim 3.2 \times 10^2 \times (\beta_c - \beta)^{-1.2} \times (4.1)^{-l_{max}} . \quad (6.2)$$

If we require these errors to be smaller than the numerical errors, we find that $l_{max} = 40$ is a safe choice for all the values of $\beta_c - \beta$ accessible with double precision. Slightly larger values are obtained for $D = 4$ and 5, which confirms that the last column of Eq. (3.4)

represents approximately the values of l_{max} above which no significant changes are observed. In conclusion, for calculations using double precision, the choice $l_{max} = 50$ is convenient and safe for the three values of D considered above.

Having an acceptable control on the susceptibility guarantees that we have an acceptable control on the higher moments, $\langle M_n^{2q} \rangle_n / 2^{qn}$ for $q > 1$, since to leading order in the volume, these quantities are dominated by the disconnected parts. The precision which can be achieved on the connected parts (which enter in the definition of the renormalized coupling constants) is a more delicate question, which is discussed in section VIII.

VII. EFFECTS OF FINITE DIMENSIONAL TRUNCATIONS ON THE HT COEFFICIENTS

In a previous publication [10], we used the truncated algorithm to calculate 800 coefficients of the high-temperature expansion of the magnetic susceptibility. We claimed that this truncation did not affect the numerical values obtained. In this section, we provide a more systematic justification of this procedure.

We examine the l_{max} -dependence of the high-temperature coefficients of the susceptibility, for dimensions 3, 4, and 5. As in section VI, we replace l_{max} with l for notational purposes. We denote the high-temperature coefficients as b_m for the m th coefficient.

For l and m large enough, we find good linear fits in l for the quantity

$$\frac{\text{Ln}((b_m - b_m^{(l)})/b_m)}{\text{Ln}(l)},$$

where $b_m^{(l)}$ is the truncated version of the exact b_m . Fig. 10 show these lines in $D = 3$, for $m = 200, 300$, and 400 . Very similar numerical values are obtained for $D = 4$ and $D = 5$. For this reason, it was impossible to display the values for the three chosen dimensions in a single graph. The graphs in $D = 4$ and $D = 5$ are similar looking and show a linear behavior as good as in $D = 3$. We can thus express the truncated coefficients as

$$b_m^{(l)} = b_m(1 - l^{-|s|l+q}), \quad (7.1)$$

where s and q are, respectively, the slope and intercept of the corresponding fitted line. For the three chosen dimensions, the lines seem to “focus” in one point close to the $l = 0$ axis. The intercepts are approximately independent of m and take the approximate values 3.4 ($D = 3$), 2.3 ($D = 4$), and 1.7 ($D = 5$). For the slopes, we find straight line fits if we plot

$$\frac{\text{Ln}(-s(m))}{\text{Ln}(m)}$$

versus $\text{Ln}(m)$ for $D = 3$, and versus m for $D = 4$ and 5 . In Figs. 11 and 12 we have used every tenth coefficient in the range from $m = 300 \dots 400$. From these fits, we find for $D = 3$:

$$s = -m^{.013\text{Ln}(m) - .22}. \quad (7.2)$$

For $D = 4$ we found

$$s = -m^{.000024m-.19}, \quad (7.3)$$

and for $D = 5$:

$$s = -m^{.000028m-.21}. \quad (7.4)$$

In $D = 3$, for example, these results show us that we need l larger than 34 for the error on b_{1000} to be less than 10^{-16} , while for $D = 4$, $l > 38$. Therefore, the value of $l = 50$ we have previously used in calculating the first 800 coefficients is more than adequate.

VIII. CALCULATION OF SUBTRACTED QUANTITIES

In this section, we discuss the numerical aspects of the calculation of subtracted quantities. We specialize the discussion to the calculation of the “dimensionless renormalized coupling constant” [12] corresponding to the 4-point function.

From Eq.(2.6), it is clear that the calculation of $R_n(k)$ allows us to determine the renormalized coupling constants. The first step in the calculation of these quantities is to extract the connected parts. In other words, we first subtract the disconnected parts from the $2k$ -point function. From a numerical point of view, this is not a trivial operation, because the subtracted quantities (connected parts) scale differently with the volume than the parts of which they are made. For instance, for $\beta < \beta_c$ and n sufficiently large,

$$\langle M_n^4 \rangle_n - 3(\langle M_n \rangle_n)^2 \propto 2^n, \quad (8.1)$$

while the individual components scale like 2^{2n} . The situation is worse if we consider the 6-point functions, where the connected part has the same scaling as Eq. (8.1) but the individual components scale like 2^{3n} . In other words, the beginning significant numbers of the individual terms do not matter for the subtracted quantities. Assuming 16 significant digits, when 2^{2n} reaches 10^{16} , we still get the subtracted parts with 8 significant digits. When 2^n reaches 10^{16} , there are no significant digits left for the subtracted part.

As a consequence, it is not always possible to stabilize the value of the connected part during as many iterations as we would like, given the study of section V. This is an interesting situation. As long as we increase the number of iterations, we get a value of the unsubtracted quantity which becomes closer to its infinite volume limit. If we represent the significant digits of a double precision number as a sequence of 16 digits written in the conventional way, we can visualize this procedure as the successive obtention of the digits on the right side of the number. Unfortunately, at the same time, the part which gets subtracted increases in magnitude. Consequently, more and more digits on the left side of the number are wasted for the evaluation of the subtracted quantities. The situation gets worse if we consider the 6 or higher point functions.

The subtracted quantities are diverging near criticality. However, it is possible to define [12] dimensionless renormalized coupling constants which have a finite limit. In the case of the four point function, the dimensionless renormalized coupling constant λ_4 is obtained by multiplying the zero-momentum connected Green’s function G_4^c by the $D + 4$ power of the renormalized mass m_R , namely

$$\lambda_4 = -G_4^c m_R^{D+4}. \quad (8.2)$$

The mnemonic for $D + 4$ is 8 (amputation of the 4 legs at zero-momentum) + $D - 4$ (the canonical dimension of the ϕ^4 bare coupling constant). We are using the notation

$$G_4^c = \lim_{n \rightarrow \infty} \frac{\langle M_n^4 \rangle_n - 3(\langle M_n \rangle_n)^3}{2^n} \quad (8.3)$$

In order to compare with field theory results, one should consider Landau-Ginzburg measures where the cut-off dependence has been restored explicitly. For instance, in $D = 3$, the definition of the functions entering in the Callan-Symanzik equations (the beta function etc.) given in Ref. [12] requires that we keep the *dimensionful* constant fixed while the cut-off goes to infinity. In other words, we need to change the *dimensionless* constant entering in $R_0(k)$ while taking the infinite cut-off limit. This delicate procedure is beyond the scope of this paper, where we emphasize the basic numerical aspect of a single calculation. As explained in the introduction, we continue using a fixed Ising measure and a single adjustable parameter (β).

The quantity λ_4 has a finite (and supposedly non-zero when $D < 4$) limit when $\Lambda \rightarrow \infty$ or equivalently when $\beta \rightarrow \beta_c$. We can thus bypass the explicit introduction of the cut-off. Taking into account that there is no wave function renormalization, or in other words that the critical exponent η is zero, we define λ_4 as the limit where n goes to ∞ of

$$\lambda_{4,n} = \frac{\langle M_n^4 \rangle_n - 3(\langle M_n^2 \rangle_n)^2}{2^n (\frac{\langle M_n^2 \rangle_n}{2^n})^{\frac{D}{2}+2}}. \quad (8.4)$$

Equivalently, with the convention of Eq. (2.9), which does not involve inverse factorials, and for the value $s = 2c^{-\frac{1}{2}}$ always used here, we obtain

$$\lambda_{4,n} = 12 \frac{a_{n,1}^2 - 2a_{n,2}}{(-2a_{n,1})^{\frac{D}{2}+2}}. \quad (8.5)$$

In practice, we pick a given relative precision Δ and we require that n is large enough to stabilize the susceptibility *and* λ_4 with a relative precision δ . The reason for requiring both conditions is that λ_4 may temporarily stabilize when the flow passes near the fixed point (and so we are still far away from the infinite volume limit), but this is signaled by the fact that the susceptibility is still growing. In summary, we require

$$\left| \frac{a_{n+1,1}}{a_{n,1}} - \frac{c}{2} \right| < \Delta \quad (8.6)$$

and

$$\left| \frac{\lambda_{4,n+1}}{\lambda_{4,n}} - 1 \right| < \Delta. \quad (8.7)$$

When these two conditions are satisfied, we check that our result for λ_4 is compatible with the expected precision, or in other words, that we have enough significant digits left in $a_{n,1}^2 - 2a_{n,2}$ to calculate λ_4 with a relative precision Δ . We thus require the additional condition

$$\left| \frac{a_{n,1}^2 - 2a_{n,2}}{2a_{n,2}} \right| > \frac{\delta}{\Delta}, \quad (8.8)$$

where δ is a typical round-off error (10^{-16} in double precision). If the additional condition is not satisfied, we lower δ and repeat the calculation. We have applied this algorithm in $D = 3, 4$, and 5 and for $-\text{Log}_{10}(\beta_c - \beta) = 2, 3, \dots, 14$.

For $D = 3$, we were able to do all the calculations with $\Delta = 10^{-6}$. We found that λ_4 reaches a limit $\lambda_4^* = 1.92786$ when $\beta \rightarrow \beta_c$. In other words, hyperscaling holds very well. Fig. 13 shows that to a good approximation

$$\lambda_4 - \lambda_4^* \simeq 1.68 \times (\beta_c - \beta)^{-0.43} . \quad (8.9)$$

In $D = 4$, we had to reduce to $\Delta = 10^{-4}$. We found that λ_4 tends to zero when $\beta \rightarrow \beta_c$. As shown in Fig. 14, we have the approximate law

$$\lambda_4 \simeq \frac{1}{-1.96 - 0.746 \times \text{Ln}(\beta_c - \beta)} , \quad (8.10)$$

which is consistent with perturbative calculations [15].

In $D = 5$, we had to reduce further to $\Delta = 10^{-2}$. We found that λ_4 tends to zero according to the approximate law

$$\lambda_4 \simeq 1.02 \times (\beta_c - \beta)^{0.507} , \quad (8.11)$$

as shown in Fig. 15. If we replace $(\beta_c - \beta)$ by Λ^{-2} , we see that our result is consistent with $\lambda_4 \propto \Lambda^{-1}$.

IX. CONCLUSIONS AND PERSPECTIVES

We have shown that the use of truncations in the Fourier transform of the recursion relation of Dyson's hierarchical model leads to systematic errors which can be suppressed more than exponentially when the dimension of the truncated space increases. We have justified the use of the truncation for calculations [10] of the high-temperature expansion. We have shown that the finite volume effects can be reduced with an exponential precision. We have found the temperature dependence of the numerical errors and explained the empirical results with a simple renormalization group argument.

The numerical errors appear as a practical aspect of the hierarchy problem. If it seems hard to believe that nature would fine-tune its fundamental parameters to produce scalar particles with masses very small compared to the Planck scale, there are also practical difficulties related to this fine-tuning. In the present context, it is quite simple to find β_c . However, this is not the end of the story: the physical quantities become numerically unstable when we reach β_c . This difficulty is not unsurmountable if we want to reach a cut-off of the order of the Planck scale which is *only* 17 orders of magnitude larger than the weak scale. We can use programming methods with enough significant digits. To take the analogy with differential equations, the problem of sensitive dependence on initial conditions can be dealt with provided that we do not evolve the system during a too-long amount of time.

The methods presented here can be applied to field theoretical calculations. The simplest one is the calculation of the renormalized mass. This quantity is crucial because it enters

into the definition of the functions appearing in the Callan-Symanzik equations [12]. For the model considered here, a possible definition of the renormalized mass is

$$m_R^2(\mu) = \lim_{L \rightarrow \infty} \frac{\Lambda^2}{\chi_\infty(\beta_c + \lambda^{-L}\mu)} , \quad (9.1)$$

where λ is the largest eigenvalue of the linearized renormalization group transformation which needs to be calculated precisely. Λ is a UV cut-off taking the value $2^{\frac{L}{D}}\Lambda_R$ where Λ_R is a scale of reference below which we are considering an effective theory. Finally, μ is a parameter which allows us to change the value of the renormalized mass. As explained in section VIII, the method can also be applied to the calculation of renormalized quantities in Landau-Ginzburg models. These calculations will be used to check the validity of the perturbative evaluations of the functions entering the Callan-Symanzik equations. In the case $D = 4$, the high-temperature expansion [17] indicates that the perturbative result [15] is very accurate.

More generally, the calculational method presented here can be used to check any kind of approximate calculation which applies to the hierarchical model.

ACKNOWLEDGMENTS

This research was supported in part by the Department of Energy under Contract No. FG02-91ER40664.

REFERENCES

- * At CERN until December 31 1997.
- [1] Y. Meurice, J. Math. Phys. **36** 1812 (1995).
 - [2] B. Bacus, Y. Meurice and A. Soemadi, J. Phys. A **28**, L381 (1995).
 - [3] K. Wilson, Phys. Rev. B. **4** 3185 (1971) ; Phys. Rev. D. **3** 1818 (1971); K. Wilson and J. Kogut Phys. Rep. **12** 75 (1974).
 - [4] K. Wilson, Phys. Rev. D **6**, 419 (1972).
 - [5] F. Dyson, Comm. Math. Phys. **12**, 91 (1969) ; G. Baker, Phys. Rev. B**5**, 2622 (1972).
 - [6] Y. Meurice and G. Ordaz J. Phys. A **29**, L635 (1996).
 - [7] P. Bleher and Y. Sinai, Comm. Math. Phys. **45**, 247 (1975) ; P. Collet and J. P. Eckmann, Comm. Math. Phys. **55**, 67 (1977) and *Lecture Notes in Physics* **74** (1978) ; H. Koch and P. Wittwer, Comm. Math. Phys. **106** 495 (1986) , **138** (1991) 537 , **164** (1994) 627 .
 - [8] Y. Meurice and G. Ordaz, J. Stat. Phys. **82**, 343 (1996).
 - [9] Y. Meurice, G. Ordaz and V. G. J. Rodgers, Phys. Rev. Lett. **75**, 4555 (1995) .
 - [10] Y. Meurice, S. Niermann, and G. Ordaz, J. Stat. Phys. **87**, 363 (1997).
 - [11] P. Collet, J.-P. Eckmann, and B. Hirsbrunner, Phys. Lett. **71B**, 385 (1977).
 - [12] G. Parisi, *Statistical Field Theory* (Addison Wesley, New-York, 1988).
 - [13] G. Baker and N. Kawashima, Phys. Rev. Lett. **75**, 994 (1995).
 - [14] There is a large amount of literature on this subject. References can be found, e.g., in *Phase Transitions, Cargese 1980*, M. Levy, J.C. Le Guillou and J. Zinn-Justin eds., (Plenum Press, New York, 1982).
 - [15] E. Brezin, J. C. Le Guillou and J. Zinn-Justin, in *Phase Transitions and Critical Phenomena* vol. 6, C. Domb and M. S. Green, eds., (Academic Press, New York, 1976).
 - [16] Y. Meurice, G. Ordaz and V. G. J. Rodgers, J. Stat. Phys. **77**, 607 (1994).
 - [17] J.J Godina, Y. Meurice and S. Niermann, preprint U. of Iowa 97-2502, CERN 97-252.

FIGURES

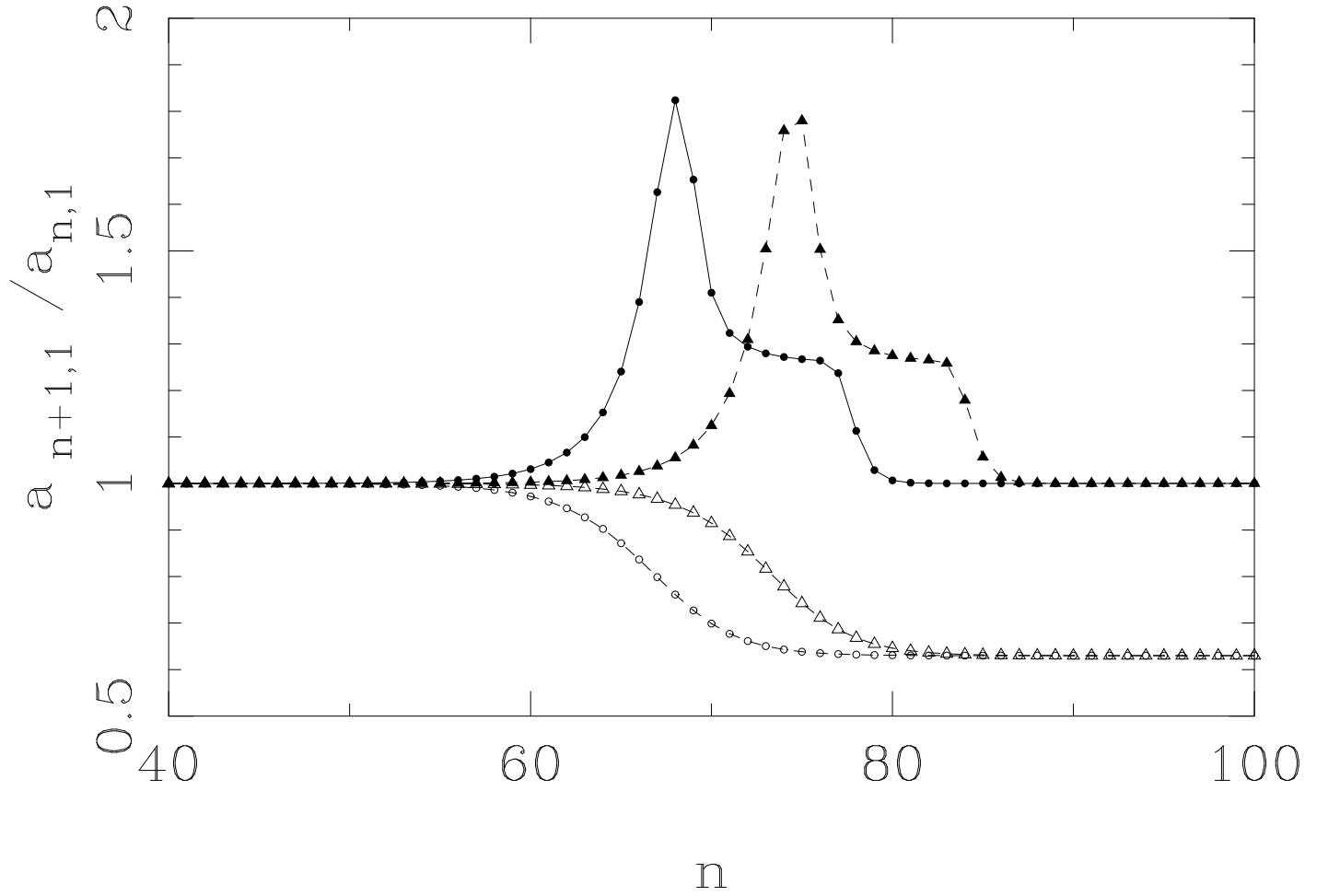


FIG. 1. $a_{n+1,1}/a_{n,1}$ versus n for $\beta = \beta_c - 10^{-10}$ (empty circles), $\beta = \beta_c - 10^{-11}$ (empty triangles), $\beta = \beta_c + 10^{-10}$ (filled circles) and $\beta = \beta_c + 10^{-11}$ (filled triangles).

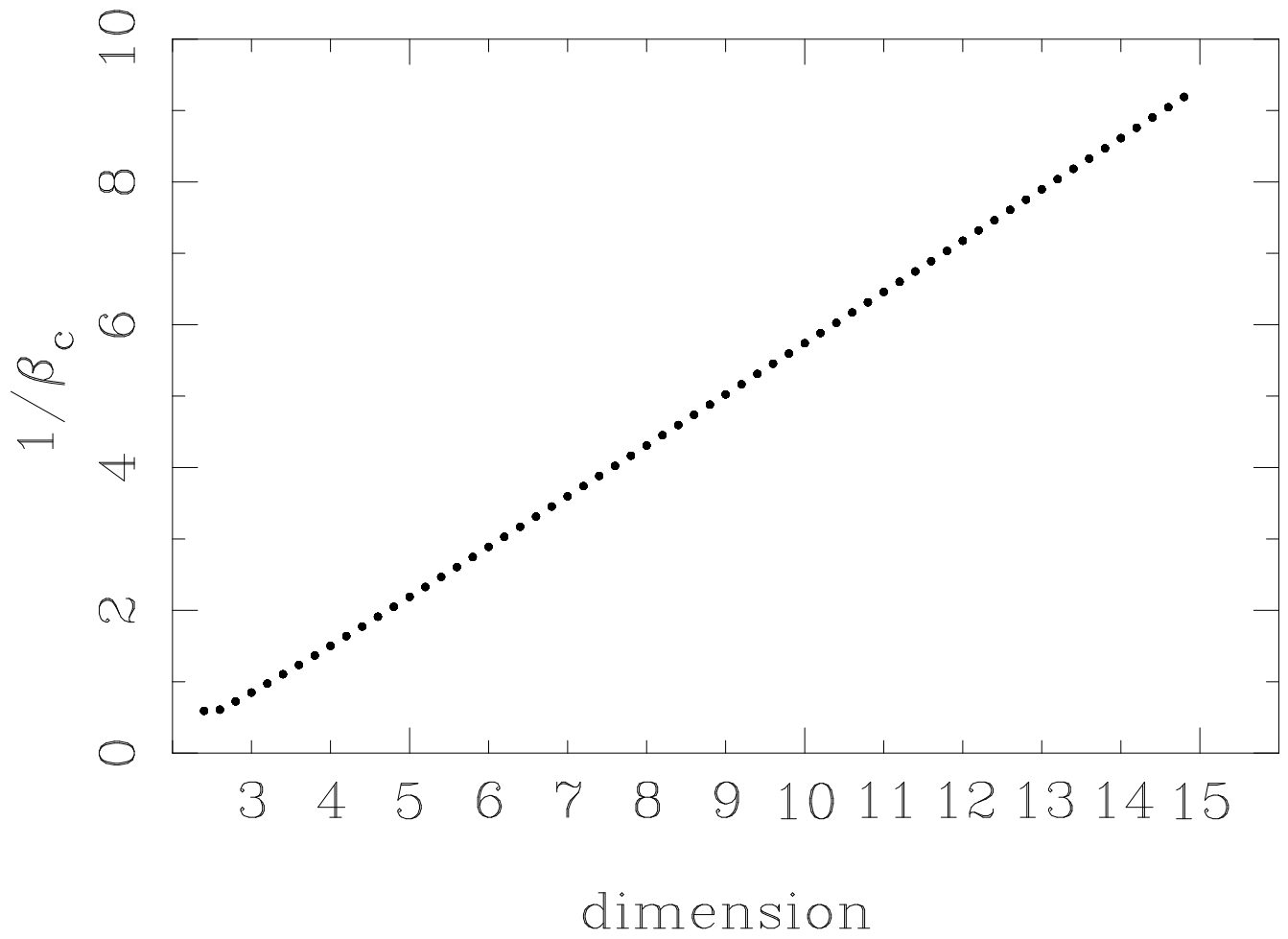


FIG. 2. $\frac{1}{\beta_c}$ versus the dimension D .

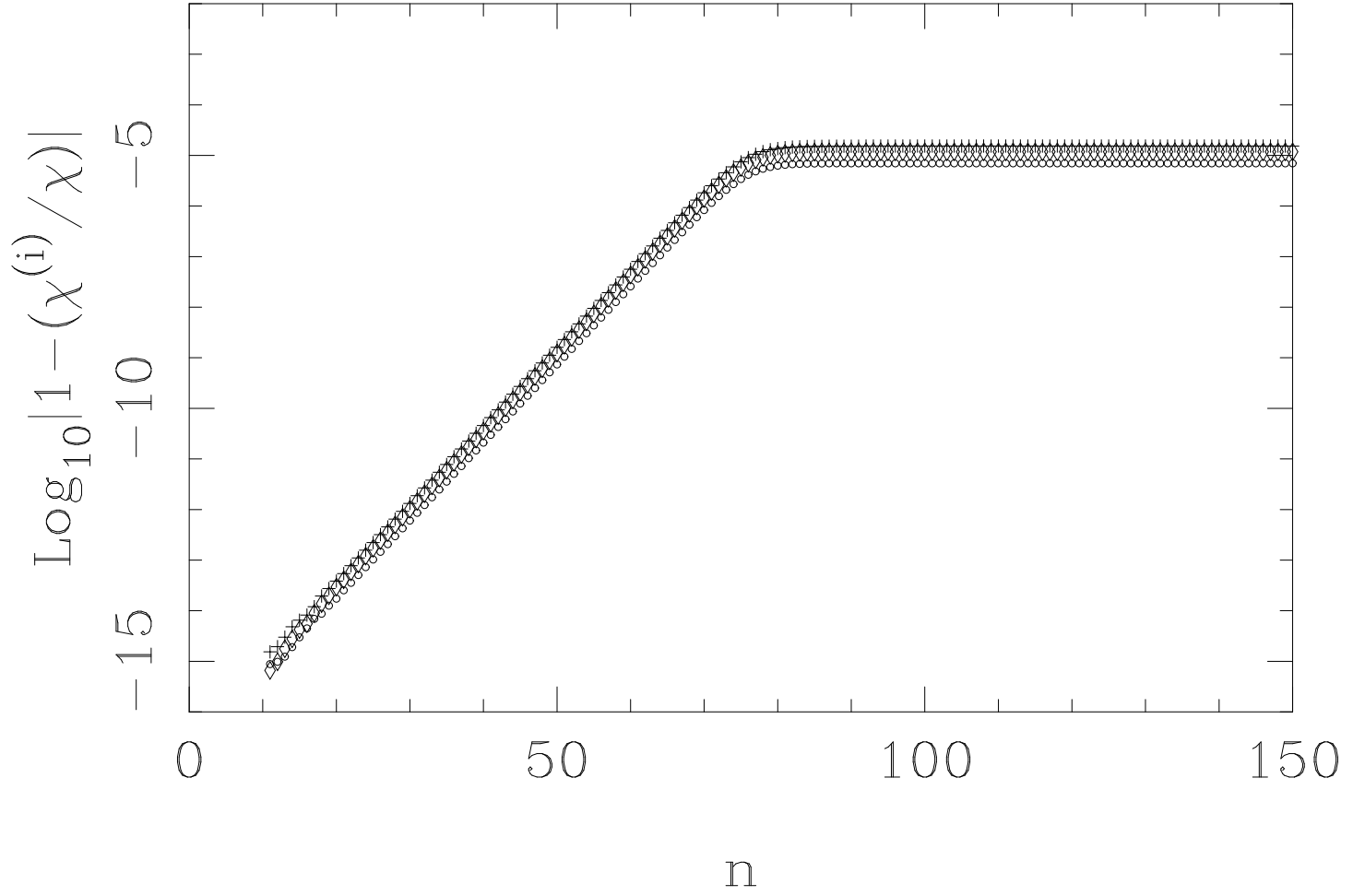


FIG. 3. Relative differences between the susceptibility calculated with the main method (χ) and three alternative methods ($\chi^{(i)}$) with $i = 1$ (crosses), 2 (diamonds) and 3 (circles) as in the text. The calculations were done in $D = 3$ and with $\beta = \beta_c - 10^{-11}$.

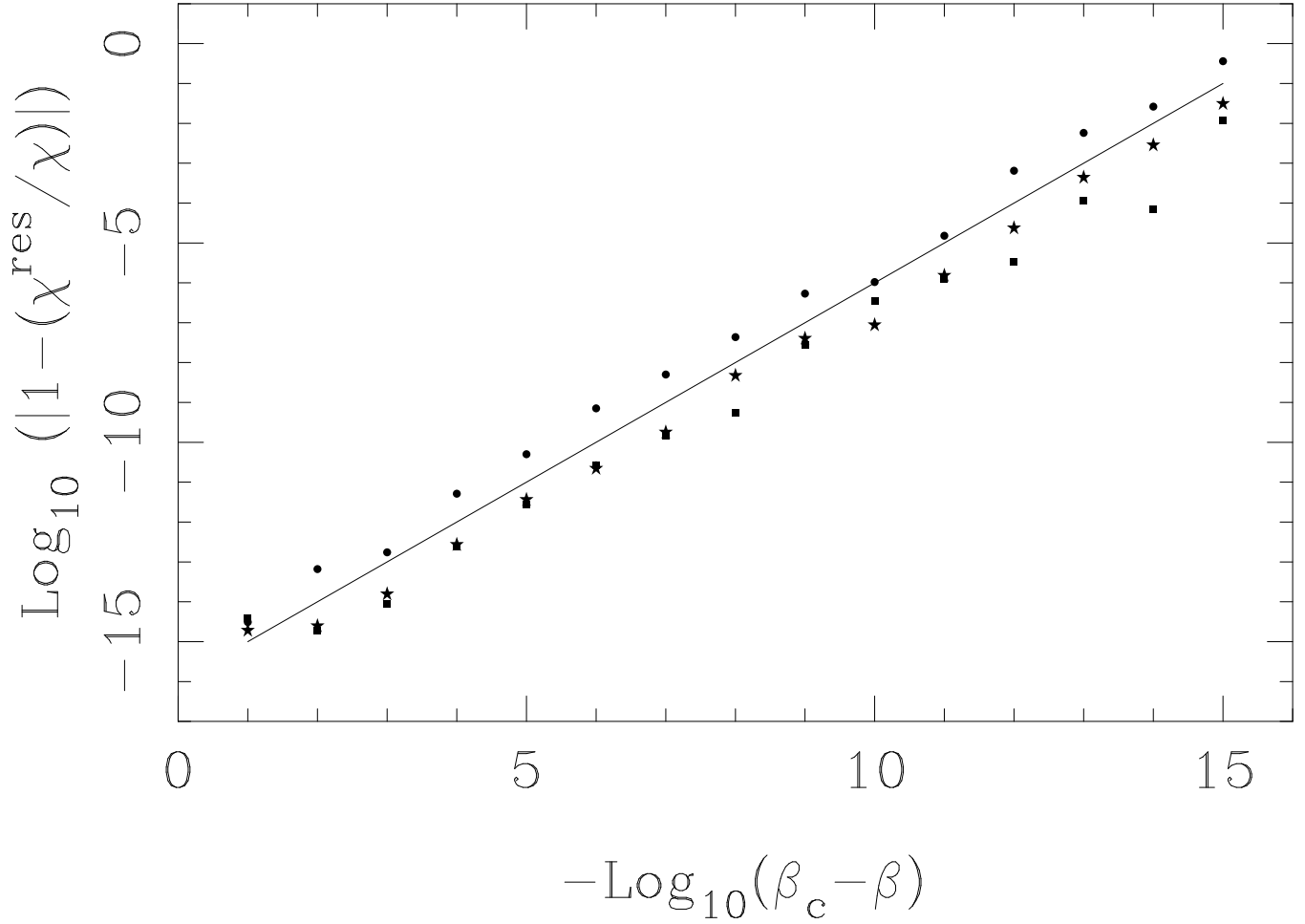


FIG. 4. Relative difference between the susceptibility calculated with the main method χ and with a rescaling χ^{res} as explained in the text versus $\beta_c - \beta$, in $D = 3$ (circles), $D = 4$ (stars) and $D = 5$ (squares).

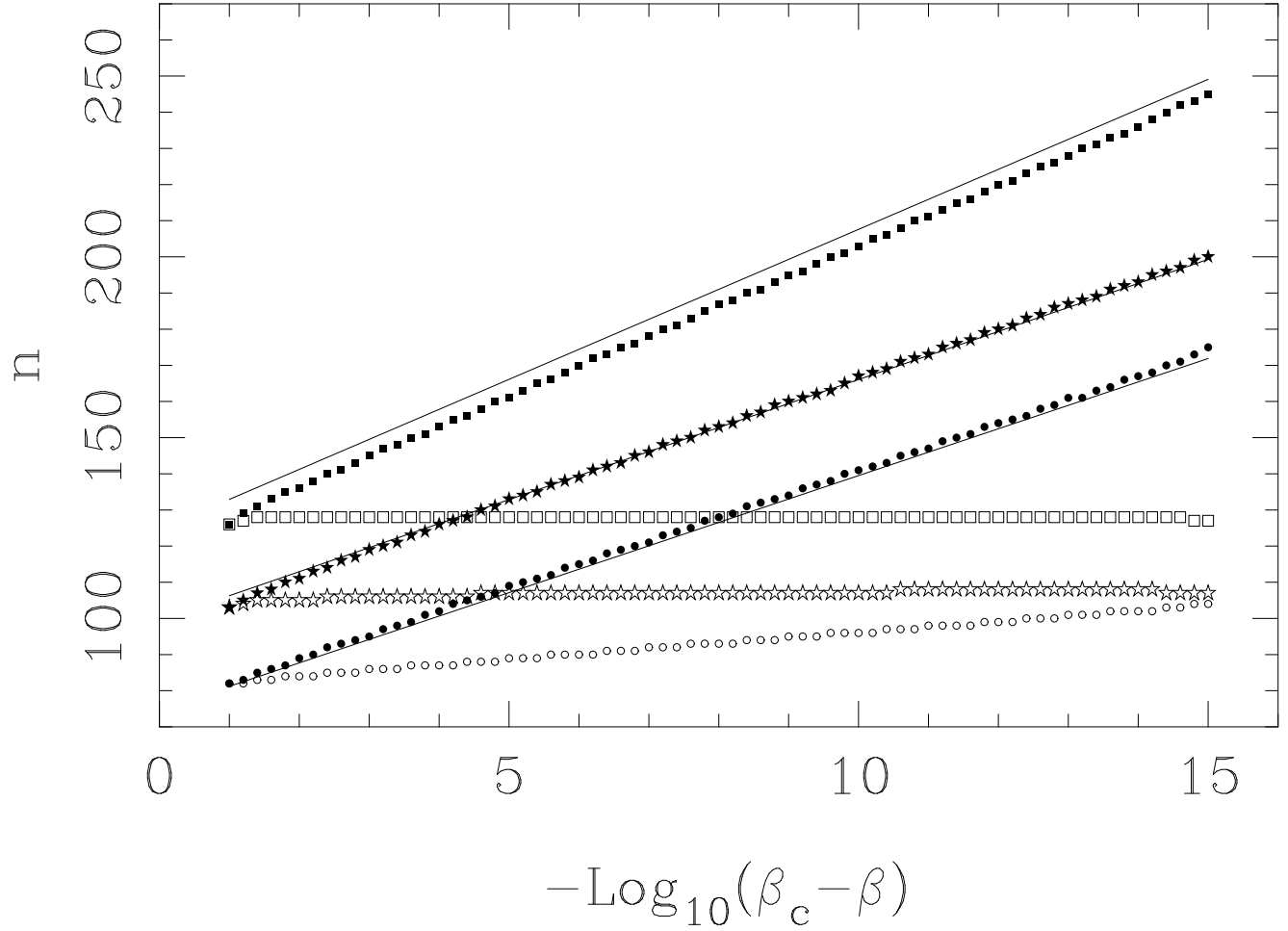


FIG. 5. $n(\beta, \Delta)$ defined in Eq.(5.2), for $D = 3$ (circles), $D = 4$ (stars) and $D = 5$ (squares). Filled symbols correspond to a fixed value $\Delta = 10^{-15}$, empty symbols correspond to a variable value $\Delta = 10^{-16}/(\beta_c - \beta)$.

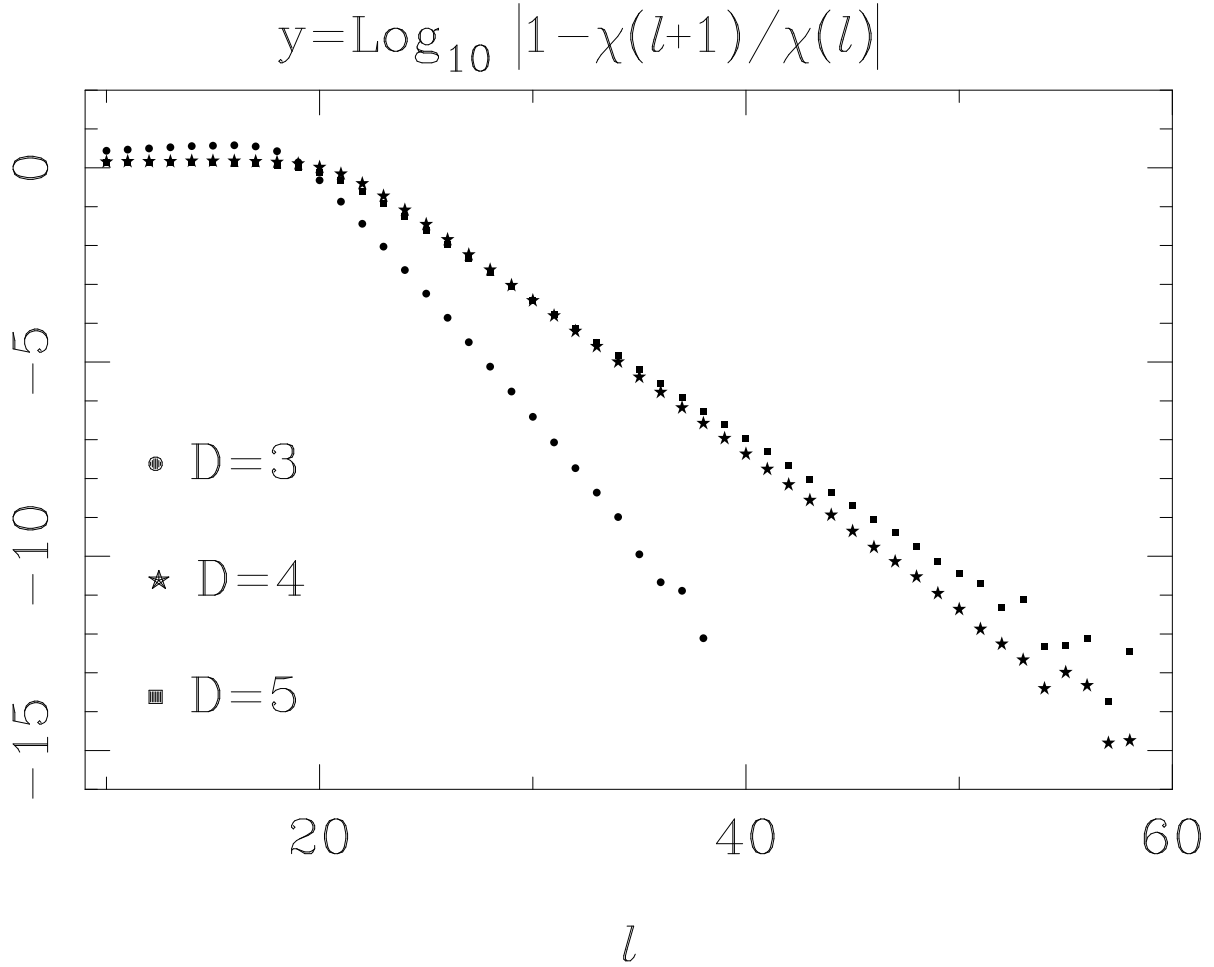


FIG. 6. Relative difference between the susceptibility calculated with $l_{max} = l + 1$ and $l_{max} = l$ in $D = 3$ (circles), $D = 4$ (stars) and $D = 5$ (squares). $\beta = \beta_c - 10^{-8}$ in the three cases.

$$y = \text{Log}_{10} |1 - \chi(l+1)/\chi(l)|$$

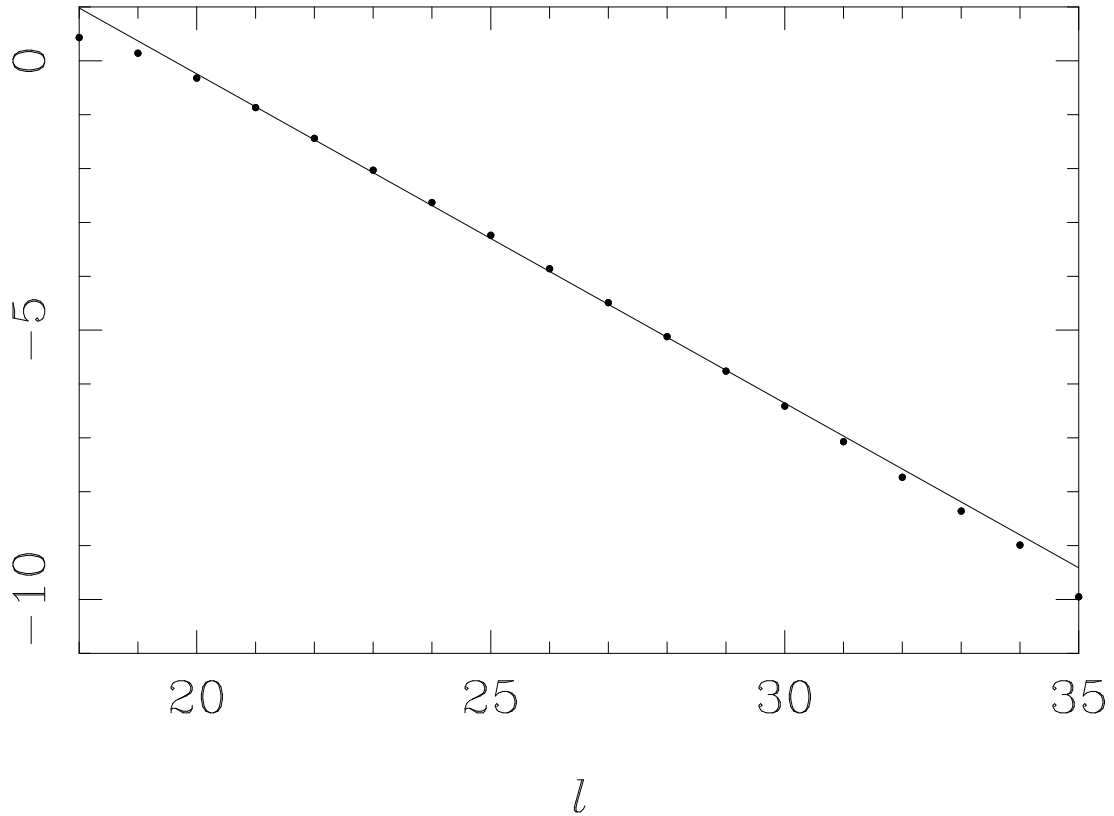


FIG. 7. Relative difference between the susceptibility calculated with $l_{max} = l + 1$ and $l_{max} = l$ in $D = 3$ (circles) and with $\beta = \beta_c - 10^{-8}$, compared with a linear fit of these points.

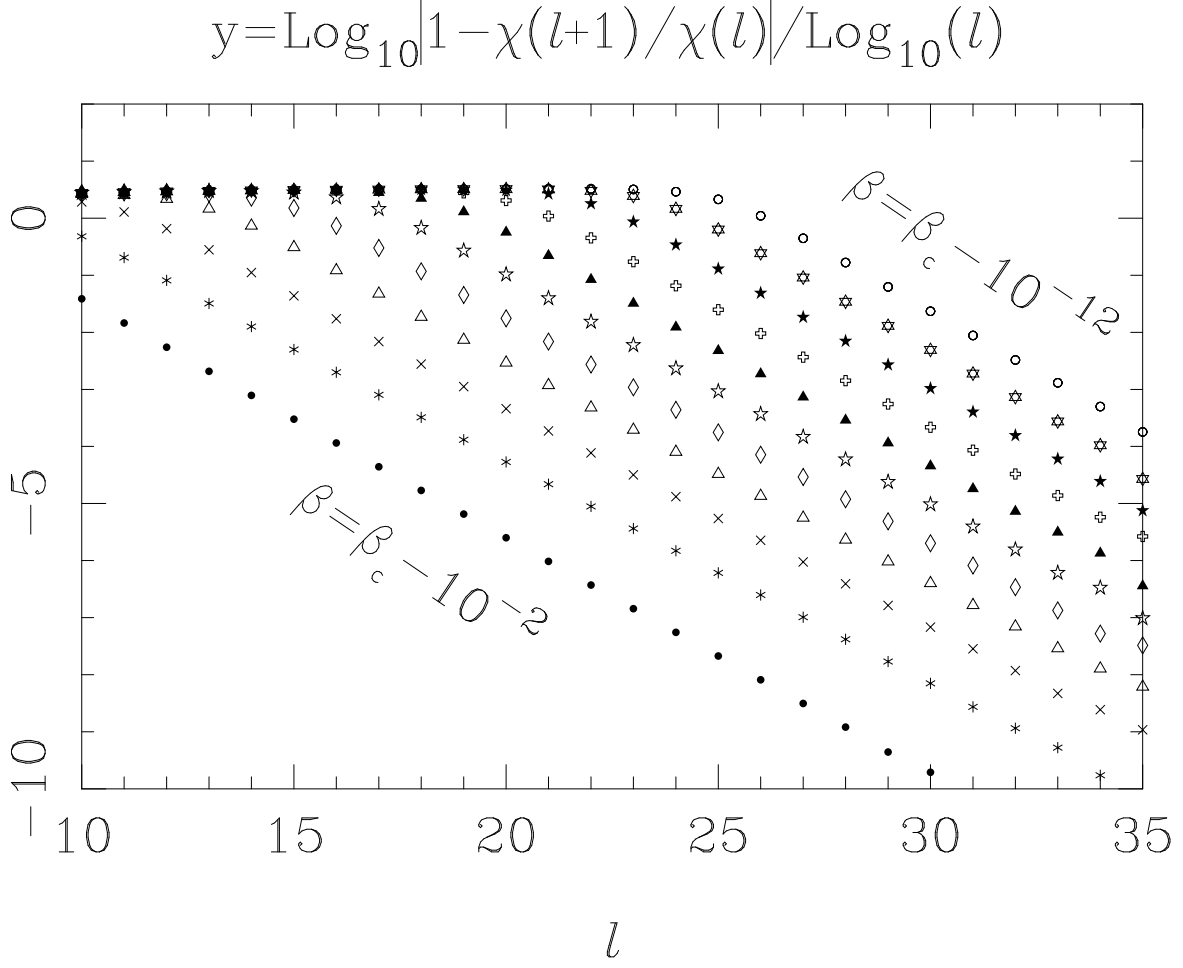


FIG. 8. Relative difference between the susceptibility calculated with $l_{max} = l + 1$ and $l_{max} = l$ in $D = 3$ with $\beta = \beta_c - 10^{-2}$ (filled circles), $\beta = \beta_c - 10^{-3}$ (asterisques), $\beta = \beta_c - 10^{-4}$ (crosses),.....up to $\beta = \beta_c - 10^{-12}$ (empty circles).

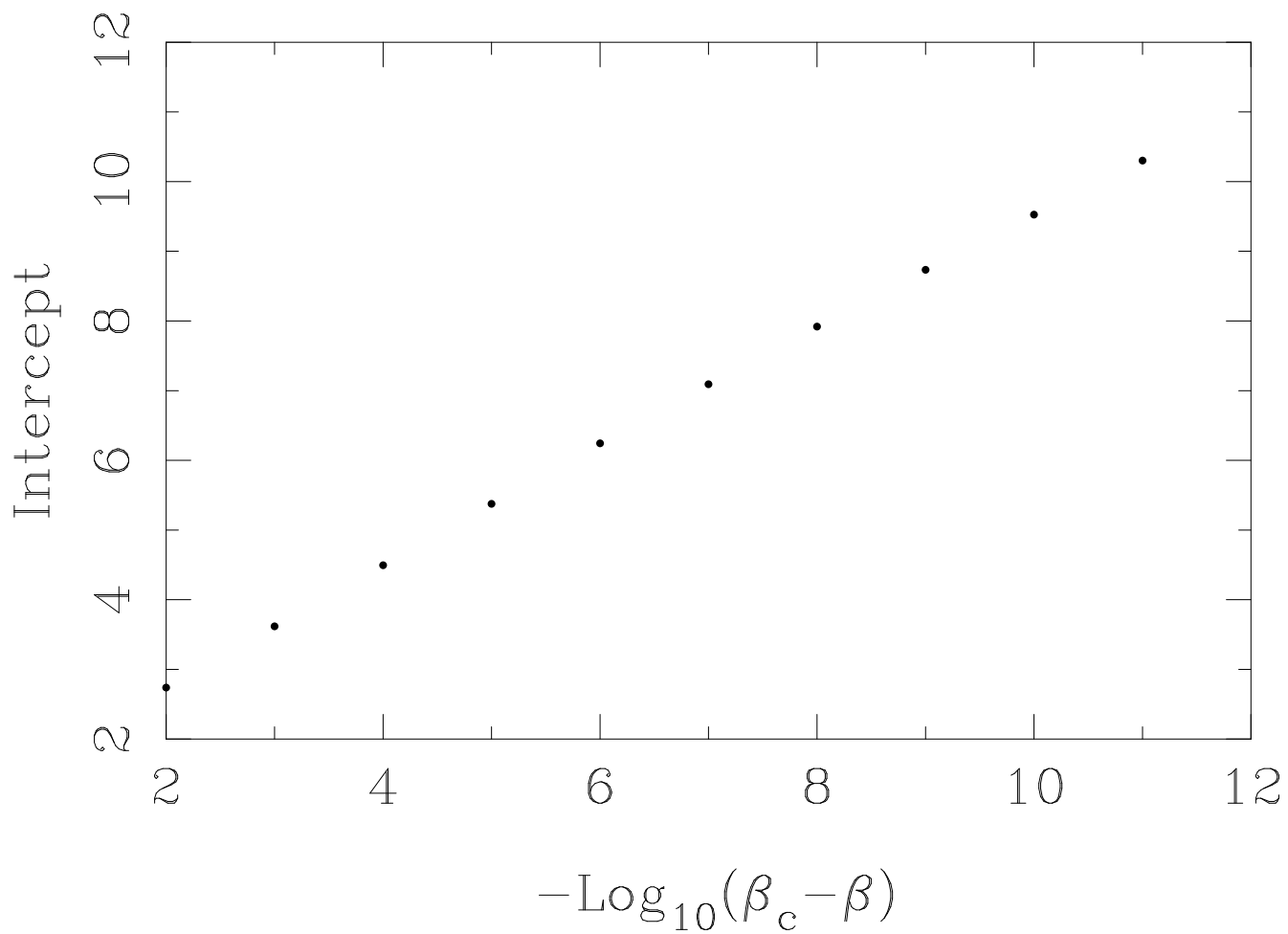


FIG. 9. Intercept of the linear fits corresponding to the linear part of Fig. 8.

l-dependence of b_m ($D=3$)

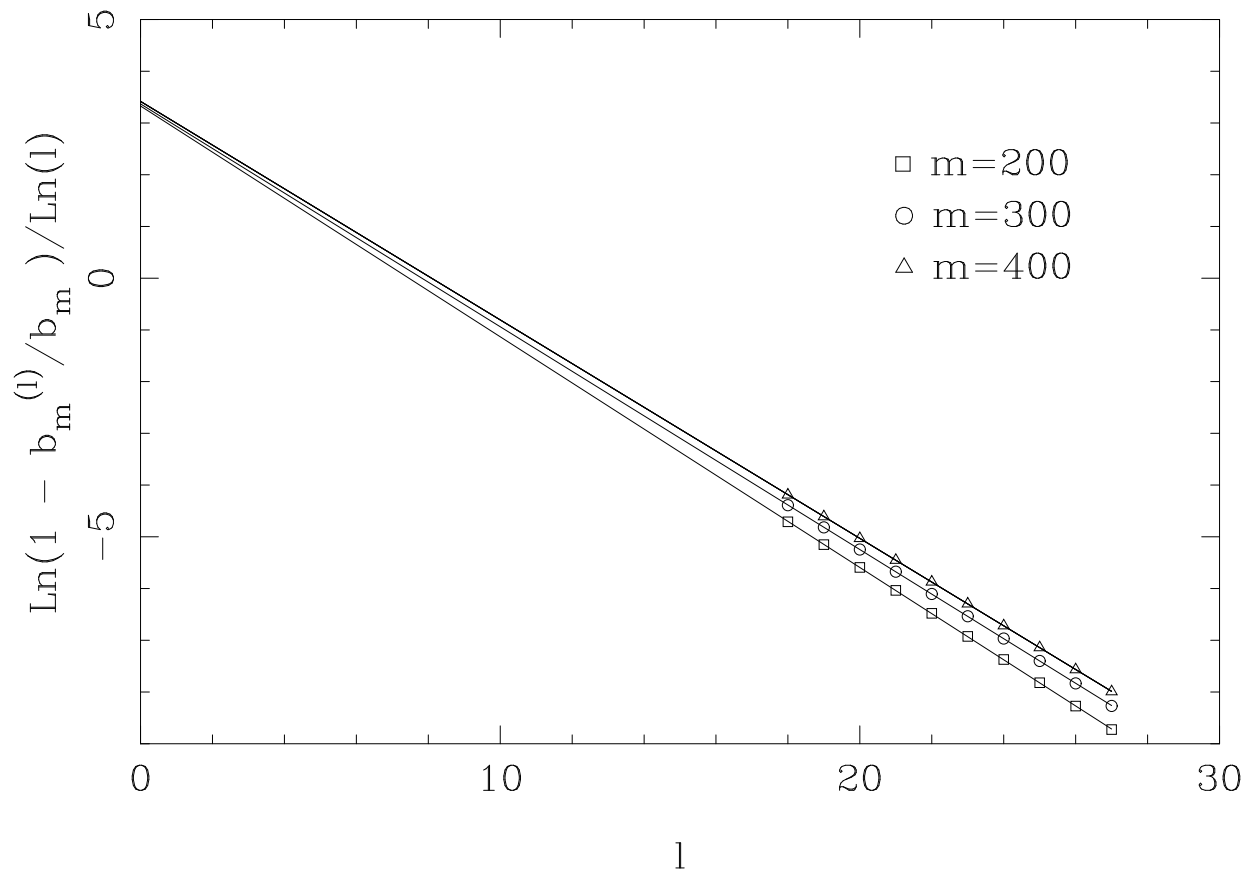


FIG. 10. Relative difference between the coefficients of the susceptibility b_m calculated with $l_{max} = l + 1$ and $l_{max} = l$ in $D = 3$ with $m=200$ (squares), $m=300$ (circles) and $m=400$ (triangles).

m-dependence of s (D=3)

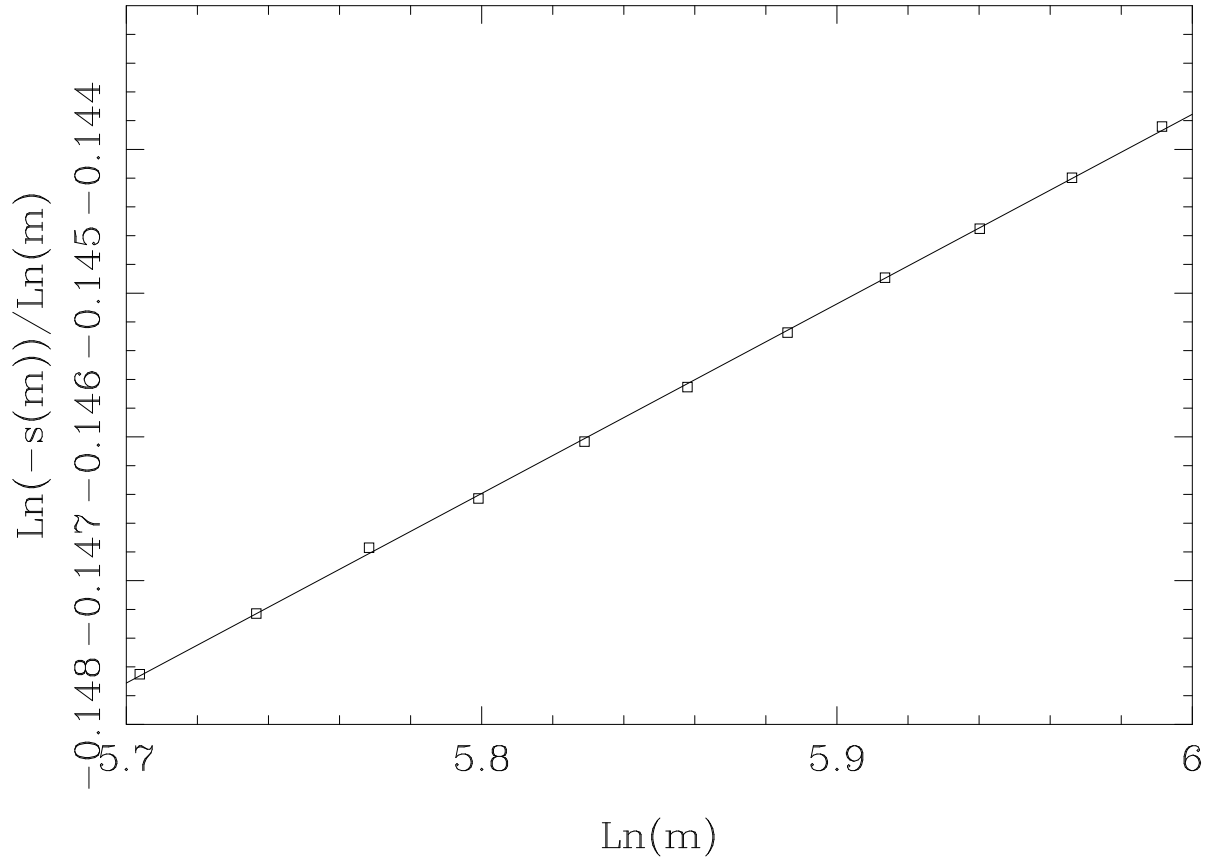


FIG. 11. $\text{Ln}(-s(m))/\text{Ln}(m)$ versus $\text{Ln}(m)$ in $D = 3$.

m-dependence of s (D=4)

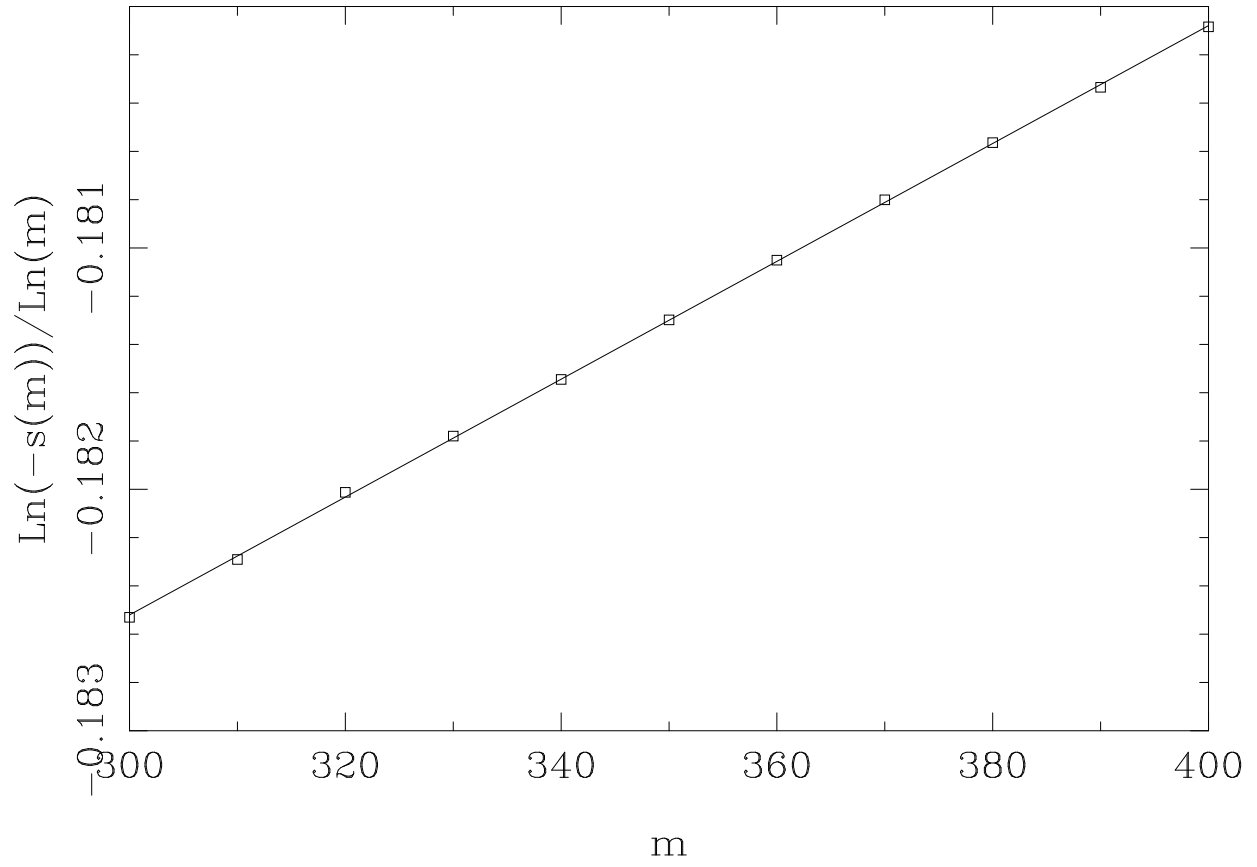


FIG. 12. $\text{Ln}(-s(m))/\text{Ln}(m)$ versus m in $D = 4$.

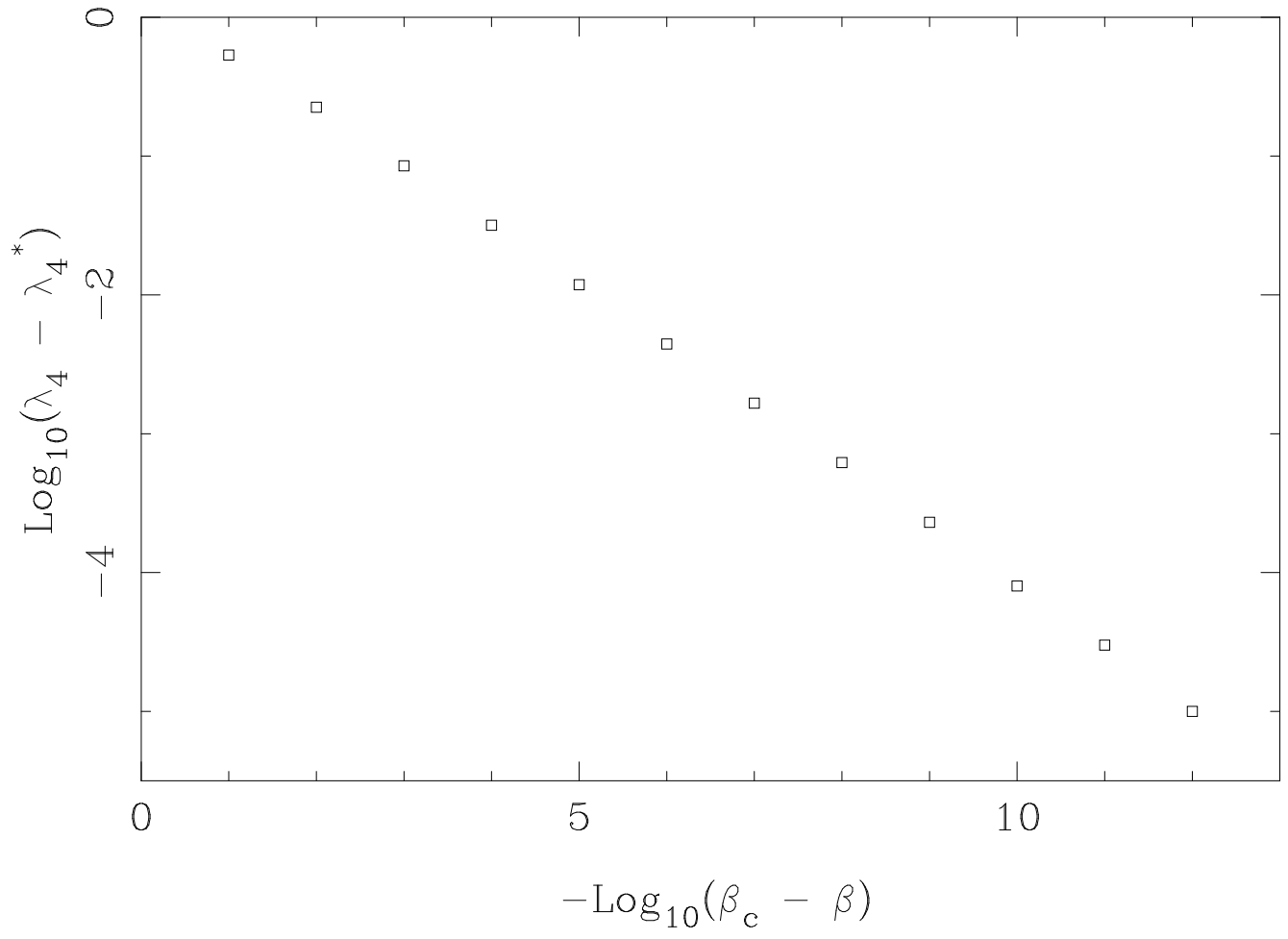


FIG. 13. $\text{Log}_{10}(\lambda_4 - \lambda_4^*)$ versus $-\text{Log}_{10}(\beta_c - \beta)$ in 3 dimensions.

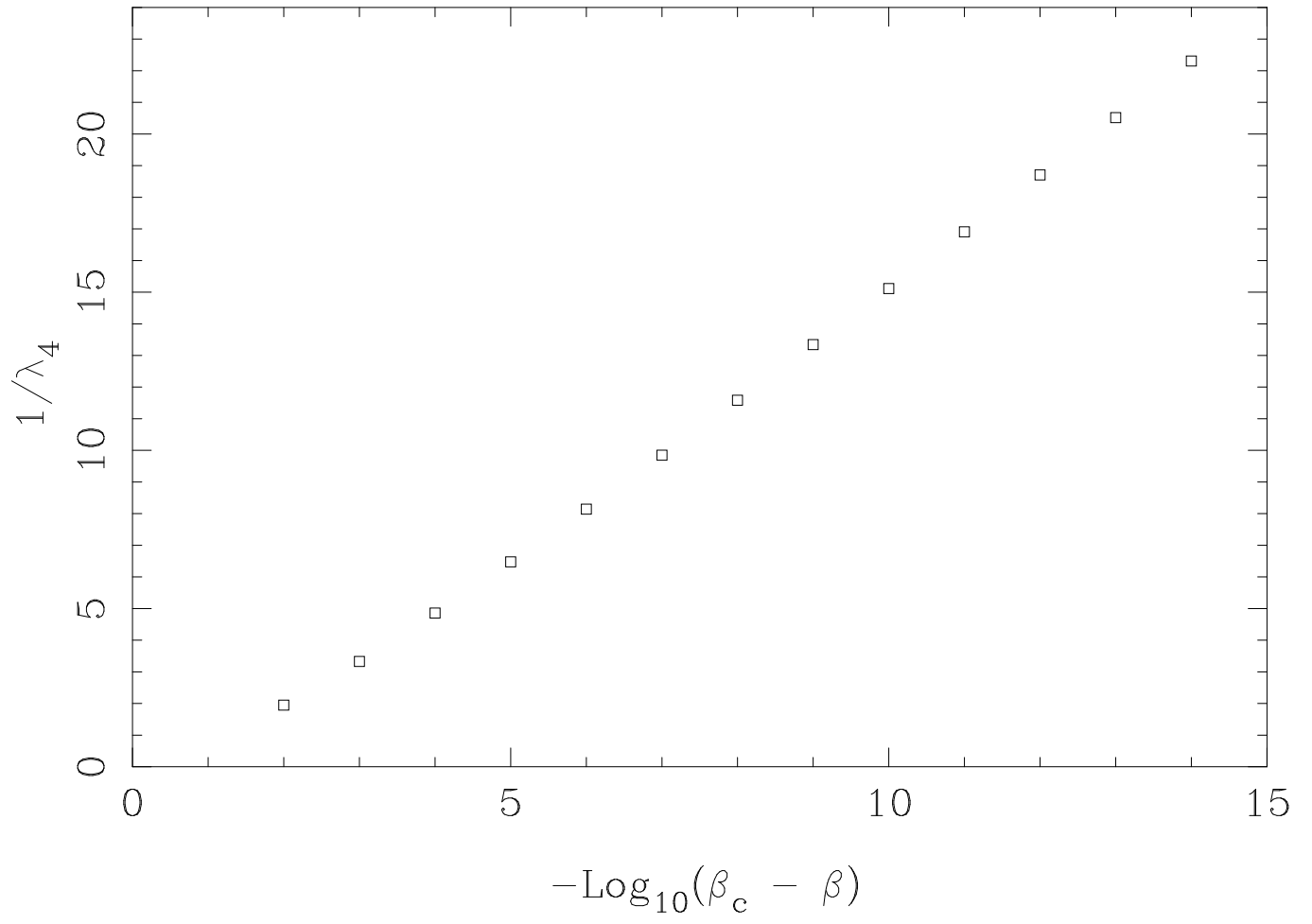


FIG. 14. $1/\lambda_4$ versus $-\text{Log}_{10}(\beta_c - \beta)$ in 4 dimensions.

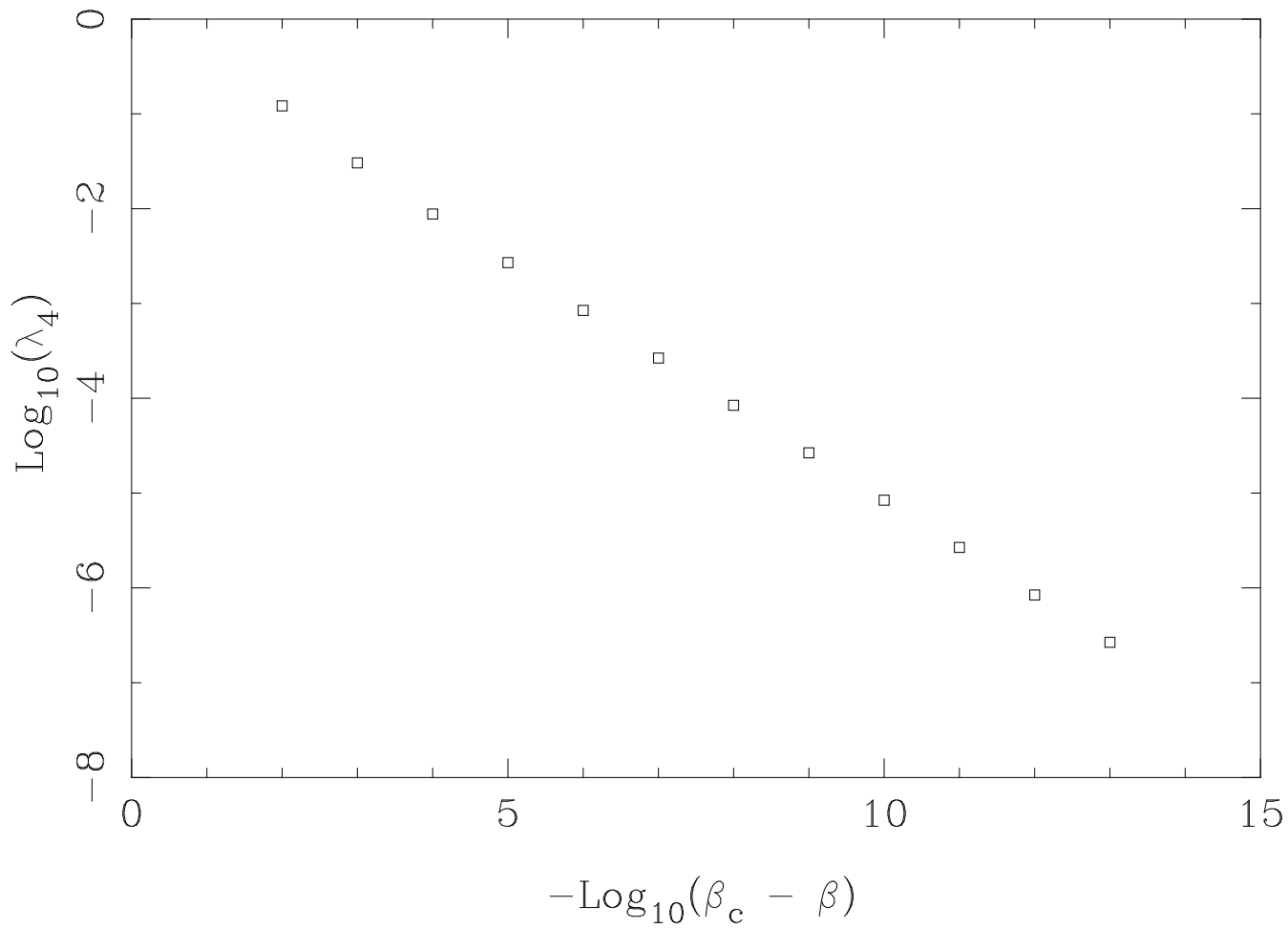


FIG. 15. $\text{Log}_{10}(\lambda_4)$ versus $-\text{Log}_{10}(\beta_c - \beta)$ in 5 dimensions.